

TOPICAL REPORT
Project No: A4373

**FINITE VOLUME MODEL FOR FORCED FLOW/THERMAL
GRADIENT CHEMICAL VAPOR INFILTRATION**

Thomas L. Starr and Arlynn W. Smith

March 1991

Report Prepared by:

GEORGIA TECH RESEARCH INSTITUTE
Georgia Institute of Technology
Atlanta, Georgia 30332

Under:
Sub-contract 19X-55901

Prepared for:

OAK RIDGE NATIONAL LABORATORY
Oak Ridge, Tennessee 37831

Managed by:

MARTIN MARIETTA ENERGY SYSTEMS, INC.
for the
U. S. DEPARTMENT OF ENERGY

Under Contract No.:
DE-AC05-84OR21400

GEORGIA INSTITUTE OF TECHNOLOGY

A Unit of the University System of Georgia
Atlanta, Georgia 30332

Georgia Tech
RESEARCH INSTITUTE



DEC 02 1991

Attachment 1

This report has been reproduced directly from the best available copy.

Available to DOE and DOE contractors from the Office of Scientific and Technical Information, P.O. Box 62, Oak Ridge, TN 37831; prices available from (615) 576-8401, FTS 626-8401.

Available to the public from the National Technical Information Service, U.S. Department of Commerce, 5285 Port Royal Rd., Springfield, VA 22161.

This report was prepared as an account of work sponsored by an agency of the United States Government. Neither the United States Government nor any agency thereof, nor any of their employees, makes any warranty, expressed or implied, or assumes any legal liability or responsibility for the accuracy, completeness, or usefulness of any information, apparatus, product, or process disclosed, or represents that its use would not infringe privately owned rights. Reference herein to any specific commercial product, process, or service by trade name, trademark, manufacturer, or otherwise, does not necessarily constitute or imply its endorsement, recommendation, or favoring by the United States Government or any agency thereof. The views and opinions of authors expressed herein do not necessarily state or reflect those of the United States Government or any agency thereof.

FINITE VOLUME MODEL FOR FORCED FLOW/THERMAL GRADIENT
CHEMICAL VAPOR INFILTRATION

Thomas L. Starr and Arlynn W. Smith

Materials Science and Technology Laboratory
Georgia Tech Research Institute
Atlanta, Georgia 30332

March 1991

Research Sponsored by the U. S. Department of Energy,
Fossil Energy
Advanced Research and Technology Development Materials Program

Report Prepared by
GEORGIA TECH RESEARCH INSTITUTE
Georgia Institute of Technology
Atlanta, Georgia 30332
under
Sub-contract 19X-55901

for
Oak Ridge National Laboratory
Oak Ridge, Tennessee 37831
managed by
MARTIN MARIETTA ENERGY SYSTEMS, INC.
FOR THE
U. S. DEPARTMENT OF ENERGY
under Contract No. DE-AC05-84OR21400

DISCLAIMER

This report was prepared as an account of work sponsored by an agency of the United States Government. Neither the United States Government nor any agency thereof, nor any of their employees, makes any warranty, express or implied, or assumes any legal liability or responsibility for the accuracy, completeness, or usefulness of any information, apparatus, product, or process disclosed, or represents that its use would not infringe privately owned rights. Reference herein to any specific commercial product, process, or service by trade name, trademark, manufacturer, or otherwise does not necessarily constitute or imply its endorsement, recommendation, or favoring by the United States Government or any agency thereof. The views and opinions of authors expressed herein do not necessarily state or reflect those of the United States Government or any agency thereof.

ENCLOSURE

EB
MASTER

TABLE OF CONTENTS

	Page
INTRODUCTION	1
FINITE VOLUME METHOD	1
Temperature	3
Pressure	4
Concentration	4
Densification	5
Computer Program	6
SPECIFICATION OF MODEL PARAMETERS	7
Analytical Grid	7
Boundary Conditions	9
Reaction Kinetics	9
Heat Flow	10
Gas Flow	11
Reactant Transport	12
SIMULATION OF CVI DENSIFICATION	12
SUMMARY AND CONCLUSIONS	18
REFERENCES	20

LIST OF FIGURES

Figure	Page
1. Region of interest is divided into finite volume elements using a cylindrical coordinate system. Values of temperature, pressure and concentration are specied at the centers of these elements.	3
2. A coarse analytical grid for the "small" ORNL CVI reactor includes six elements in the radial direction and eleven in the vertical. The preform area is divided into a 5x5 grid.	9
3. For "baseline" conditions the preform density increases linear with time and the inlet pressure exceeds 200 kPa after seven hours. . .	14
4. The final density profile for "baseline" conditions shows little densification near the cool face of the preform.	15
5. Reducing the hot face temperature increases process time (top) but produces little improvement in density uniformity (bottom). . . .	17
6. Reducing the MTS concentration increases the process time in inverse proportion (top) but gives no change in the density profile. . . .	18
7. Reducing the overall flow rate give a much longer process time (top) and produces much improved density uniformity (bottom).	19
8. Using the linear surface area relation with "baseline" conditions gives longer process time (top) and more uniform densification (bottom).	20

INTRODUCTION

The forced flow/thermal gradient chemical vapor infiltration process (FCVI) has proven to be a successful technique for fabrication of ceramic matrix composites^{1,2,3}. It is particularly attractive for thick components which cannot be fabricated using the conventional, isothermal method (ICVI).

Although it offers processing times that are at least an order of magnitude shorter than ICVI, FCVI has not been used to fabricate parts of complex geometry and is perceived by many to be unsuitable for such components. The major concern is that selection and control of the flow pattern and thermal profile for optimum infiltration can be a difficult and costly exercise. In order to reduce this effort, we are developing a computer model for FCVI that simulates the densification process for given component geometry, reactor configuration and operating parameters. Used by a process engineer, this model can dramatically reduce the experimental effort needed to obtain uniform densification.

A one-dimensional process model, previously developed, has demonstrated good agreement with experimental results in predicting overall densification time, density uniformity, backpressure increase during processing and the effect of various fiber architectures and operating parameters on these process issues⁴. This model is fundamentally unsuitable for more complex geometries, however, and extension to two- and three-dimensions is necessary. This report outlines our application of the "finite volume" method to model FCVI and gives examples of its use with the reactor geometry similar to that used at the Oak Ridge National Laboratory (ORNL).

FINITE VOLUME METHOD

The FCVI process involves transport and conservation of energy, momentum and mass. The physical laws governing these processes can be expressed as a system of differential equations. While these equations offer the desired simulation of the infiltration process, an analytical solution is possible only for simple geometries and boundary conditions. For the more general situation - where our interest lies - a numerical approach is necessary. One such technique, the "finite volume" method, has proven successful for modeling a wide range of processes involving chemical reaction and heat and fluid flow⁵. We have adopted this method for our simulation of the FCVI process.

In the finite volume method, the region of interest is divided into an orthogonal array of volume elements. Figure 1 illustrates one such volume element, in a cylindrical coordinate system. A value for a process parameter

"Research sponsored by the U.S. Department of Energy, Fossil Energy AR&TD Materials Program, DOE/FE AA 15 10 10 0, Work Breakdown Structure Element GT-1(A)"

(temperature, pressure or concentration) is specified at a grid point located at the center of each volume element. This array of discrete values approximates the real, continuous variation of the parameter over the region of interest.

In the steady-state, the value of a parameter at each grid point is related to its neighboring values utilizing the conservation principle. For temperature, as an example, the heat flow into and out of the volume element (flux) is required to balance any heat generation or absorption within the element (source). This relationship produces a system of linear equations, one equation for each grid point. The solution of this set of equations produces the values of the parameter at each grid point.

The flux term in the conservation equations has the general form,

$$flux = uAG - D \frac{dG}{dx} \quad (1)$$

where G is a system parameter, such as temperature, u is the flow velocity in the x-direction through a face of the volume element, A is a constant related to the "convective" flux and D is a constant related to the "diffusive flux."

The source term in the conservation equations can have many forms but it is useful to express it as an explicit linear function of the system parameter, that is,

$$source = S_c + S_p G \quad (2)$$

where S_c and S_p are constants. In actual practice, S_c and S_p can depend on the system parameter so that this convention allows inclusion of non-linear source contributions, such as a second-order reaction.

For the FCVI process the important parameters include temperature, pressure and concentration of chemical species. Flux and source terms are associated with each parameter. For temperature, flux terms include heat conduction and convection. The heat of reaction is a source term for temperature but is very small and we do not include this in our model. For pressure, the flux term consists of viscous flow as expressed by Darcy's Law. Again, the source term resulting from chemical reaction is very small and is neglected. For concentration of chemical species, flux terms include diffusion and convection. The source term, production or depletion through chemical reaction, is of central importance and is included.

In order to solve the system of equations generated by the conservation principle, boundary conditions must be specified at every grid point on the edge of the region of interest. In general, either the value of the system parameter or the value of the flux is specified. Selection of the region of interest is

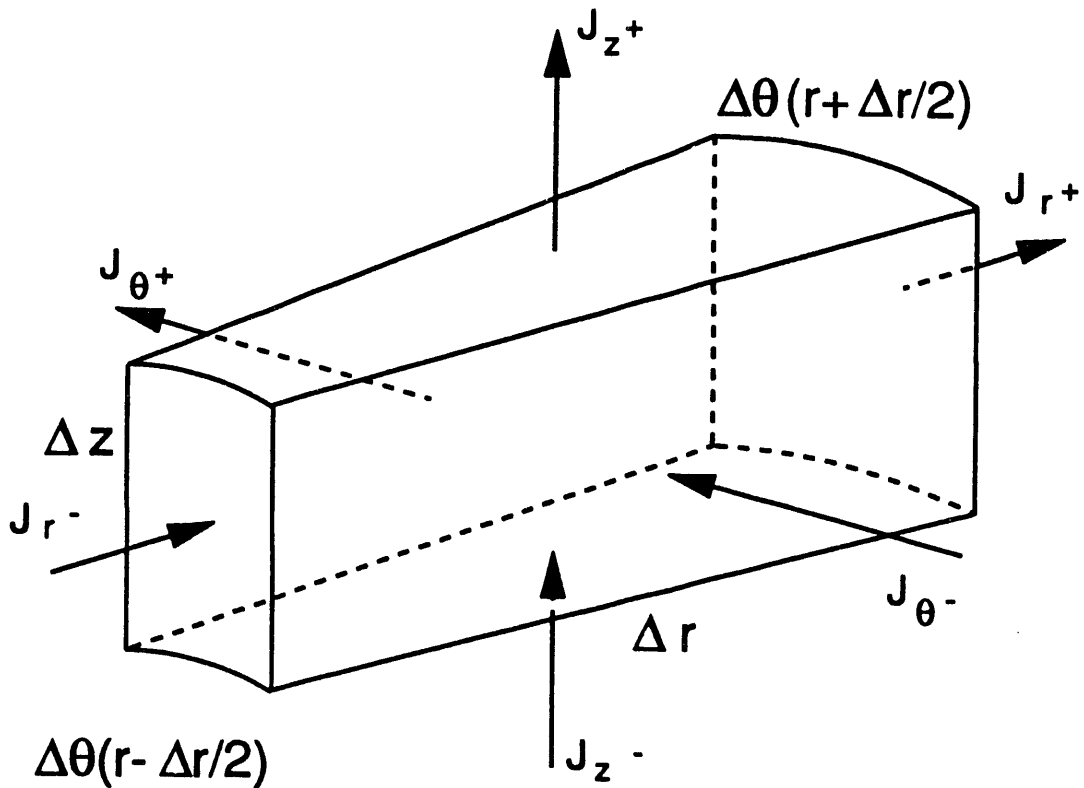


Figure 1. Region of interest is divided into finite volume elements using a cylindrical coordinate system. Values of temperature, pressure and concentration are specified at the centers of these elements.

influenced, to a great extent, by the need to have well determined boundary conditions.

Mathematically, modeling of temperature, pressure and concentration are identical problems. They differ only in the values of the parameters and constants, the form of the source term and the boundary conditions.

Temperature

For the temperature problem, the diffusive flux in Equation 1 corresponds to thermal conduction, with the constant, D , equal to the thermal conductivity.

The region of interest for the FCVI model will include volume elements that consist of different materials and, thus, different thermal conductivities. Some of these materials, such as the graphite used to construct the preform holder, remain unchanged as infiltration proceeds. The preform, however, changes dramatically in density during the process and its thermal conductivity changes as a consequence. Furthermore, for a cloth lay-up preform, the thermal conductivity is expected to be different parallel and perpendicular to the cloth layers. Provision for density dependent, anisotropic transport properties has been included in the CVI model.

The convective flux for temperature is due to heating of the cool gas as it moves through the preform and the coefficient, A , is equal to the heat capacity of the gas. For hydrogen and for gas flow rates used at ORNL, the convective contribution is only about 5% of the total heat flux through the preform.

Pressure

For pressure, the diffusive flux corresponds to viscous flow through a porous medium as expressed by Darcy's Law,

$$F = \frac{K}{\mu V_m} \frac{dP}{dx}$$

where F is the molar flux (moles/s/cm²), V_m is the molar volume of the gas, μ is the gas viscosity, and K is the permeability. Permeability depends only on the structural properties of the porous medium while μ and V_m depend only on the gas. Like thermal conductivity, gas permeability is expected to be density dependent and may be anisotropic for certain preform architectures.

There is no convective flux term for pressure in our model. This assumption corresponds to the "potential flow" approximation in fluid dynamics which neglects contributions due to gas inertia and buoyancy. While not accurate for gas flow in open reactors or ducts, this model corresponds exactly to pressure driven flow through semi-permeable bodies as is our case.

Concentration

For concentration modeling the diffusive flux term corresponds to gas phase diffusion. The effective diffusion coefficient will depend on the nature of the chemical species, the total pressure and the preform microstructure. For a porous solid the effective diffusion coefficient can be expressed,

$$D_e = \frac{Dp}{r} \quad (3)$$

where D is the Fickian or the Knudsen diffusion coefficient for the chemical species in the gas mixture, p is the fraction porosity in the porous body and r is a "tortuosity" factor. For FCVI, normally run near ambient pressure, ordinary, or Fickian, diffusion is appropriate and the value of D can be obtained from chemical engineering tables or from kinetic theory formulas. The porosity is easily calculated from the density, but the tortuosity depends on microstructure in a complex way. For anisotropic materials, the tortuosity may be different in different directions, giving an anisotropic effective diffusion coefficient.

The convective flux term corresponds to movement of the reactive species in the overall gas flow. For concentration expressed as mole fraction and flow velocity as molar flux, the convection coefficient, A , in Equation 1 is unity. For typical FCVI flow rates the convective flux through a volume element is much larger than the diffusive flux.

The source term for concentration corresponds to the reaction rate of the chemical species within the volume element. For surface deposition reactions the volumetric reaction rate, R_v , can be expressed as,

$$R_v = R_s S_v$$

where R_s is the reaction rate per unit of solid surface area and S_v is the surface area per unit volume within the porous material. R_s can be determined from chemical vapor deposition (CVD) experiments on flat substrates, with proper allowance for mass transport effects. S_v depends on the microstructure of the porous composite and varies with initial fiber size and geometry and volume fraction in the preform, and with the composite density as this increases during infiltration. Obviously, S_v must go to zero as the density increases to near 100%.

Densification

The above formulation of the finite volume model results in a steady-state solution, giving the temperature, pressure and concentration at one moment in time. As part of this solution we also obtain the molar deposition rate for each volume element. Using the stoichiometry of the deposition reaction and the molecular weight, M , and density, ρ , of the product we can convert this to a densification rate,

$$R_d = \frac{nR_v M}{g}$$

where n is the number of moles of product for each mole of reactant and R_d is the increase in the volume fraction of solid per unit time. For a given increment of time, Δt , the new density can be calculated by linear extrapolation,

$$d(t+\Delta t) = d(t) + R_d(t)\Delta t$$

This explicit formulation for densification is reasonably accurate for small time increments or when the densification rate, R_d , is reasonably constant with time. However, at near full density, where the surface area and, thus, the deposition rate, goes to zero, this method can produce a relative density greater than 100%. In order to avoid this problem, we employ an implicit formulation for densification,

$$d(t+\Delta t) = d(t) + R_d(t+\Delta t)\Delta t$$

where R_d is calculated using the steady-state temperature, pressure and concentration values but with the surface area function, S_v , for the new density. This formulation requires an iterative solution method but gives a smooth approach to full density with even relatively coarse time steps.

With new densities for each volume element, new values of the transport coefficients are calculated and new steady-state values for temperature, pressure and concentration are obtained. With multiple time increments we get a series of "snapshots" of the infiltration process. This iteration process can be continued for an arbitrary period but is usually terminated at some set value of composite density or inlet pressure.

Computer Program

The finite volume model outlined above has been incorporated into a FORTRAN computer program. Input to this program includes the geometry of the CVI reactor, boundary conditions for temperature, pressure and concentration, and a series of time increments. Built into the program are routines for estimating the transport coefficients (thermal conductivity, gas permeability, etc.) and kinetic factors for the reactants involved in the particular CVI system. This part of the model is continually evolving as better understanding is gained.

The program uses an iterative, line-by-line method for solving the systems

of linear equations. Solutions for temperature, pressure and concentration are obtained separately but this procedure is iterated until the solutions are consistent. Thus, temperature dependence of the gas flow and flow dependence of the temperature profile are properly calculated. For each time step values of temperature, pressure, concentration, density and the flow vectors for each grid point are written to a file. These results can be analyzed and displayed using stand-alone data analysis and graphics display software packages.

SPECIFICATION OF MODEL PARAMETERS

The CVI model will always produce a simulation of the CVI process. Whether this simulation matches the actual, experimental process depends critically on accurate specification of transport properties and reaction kinetics, and on proper selection of boundary conditions. Ongoing experimental efforts at Georgia Tech and at ORNL are directed toward better understanding of these factors for SiC/Nicalon composites. It is somewhat premature to expect to accurately simulate the infiltration process.

It is useful, however, to exercise the model with estimated properties so as to check for qualitative agreement with experimental observations and to gain insight into the process itself.

Analytical Grid

Since the CVI reactors at ORNL have cylindrical symmetry, a 2-D model in cylindrical coordinates is appropriate for simulation of the infiltration process. An analytical grid for the "small" ORNL CVI reactor is shown in Figure 2. This grid includes six elements in the radial direction and eleven in the vertical. The preform area itself is divided into a 5x5 grid. The additional volume elements represent parts of the preform holder and gas injector. The physical boundaries between the preform and holder coincide with boundaries between volume elements. The finite volume method has been developed to properly handle such discontinuities where the transport properties can vary by orders of magnitude⁵. This allows use of a relatively coarse grid.

Four types of volume element are used to specify the system. A free space element is used for the gas inlet up to the preform. A graphite element is used for the preform holder and gas injector. A porous graphite element is used for the cover plate. A preform element is used for the preform region. Transport properties for each of these types of elements must be specified.

Boundary Conditions

Temperature, pressure and concentration boundary conditions must be

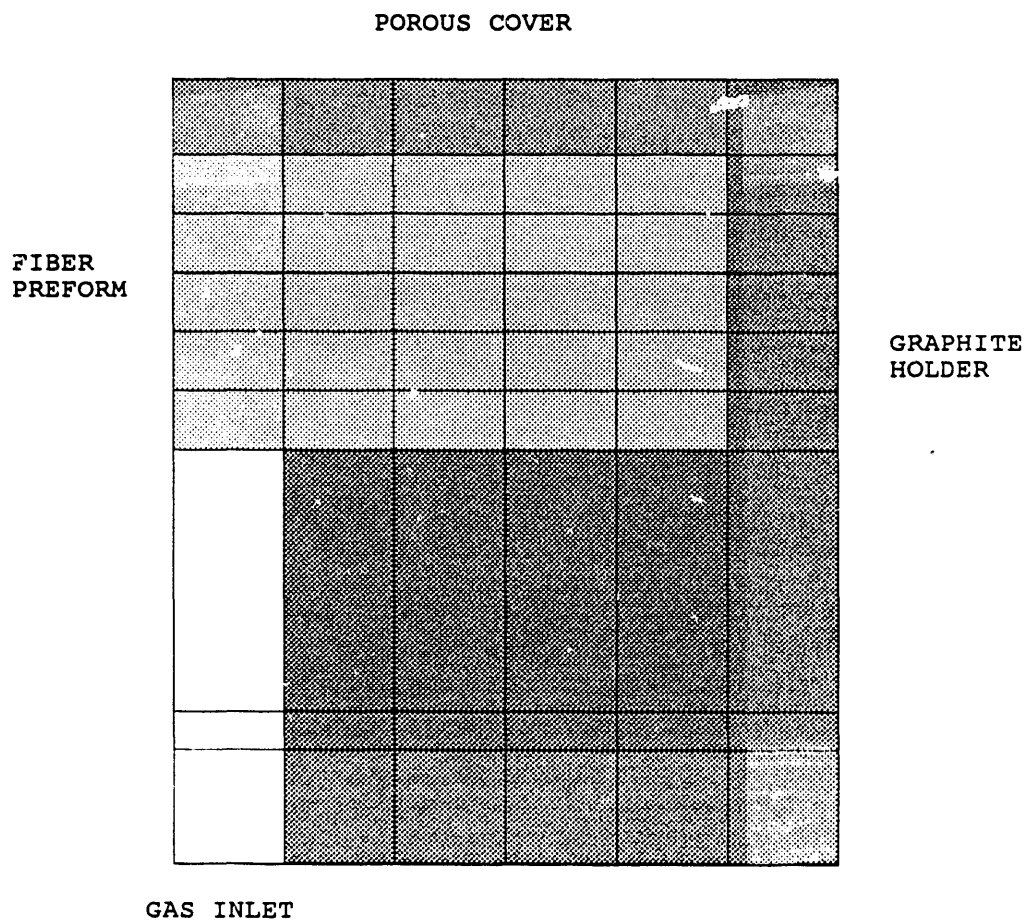


Figure 2. A coarse analytical grid for the "small" ORNL CVI reactor includes six elements in the radial direction and eleven in the vertical. The preform area is divided into a 5x5 grid.

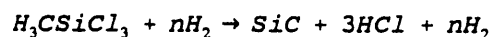
specified along each boundary of the model. For temperature the top and bottom boundary conditions are well determined. The reactor hardware is designed to maintain constant temperatures at the gas injector and at the upper surface of the lid. The thermal boundary condition at the radius is not so well defined due to the complexity of the furnace and reactor configuration. For now, we specify this as an adiabatic wall, i. e. no net heat flux through this boundary. This is in rough agreement with embedded thermocouple measurements which show only a small temperature gradient in the radial direction⁶.

The pressure boundary conditions are well defined. The top of the lid is set at constant ambient pressure of 100 KPa. All other boundaries are set as "adiabatic" walls (no flow) except for the inlet element. The inflow here is set to match the experimental gas flow.

The concentration boundary conditions also are well defined. The inflow boundary is set at the mole fraction corresponding to H₂:MTS composition. All other boundaries are set as "adiabatic" walls, i.e. no diffusion through these boundaries.

Reaction Kinetics

For CVI of silicon carbide matrix composites using methyltrichlorosilane (MTS) the overall reaction is,



showing one mole of silicon carbide for each mole of MTS reacted. In reality, the reaction is more complex with a number of intermediate reactions and reaction products. In spite of this complexity, experimental measurements of deposition rate onto fibers⁷ fit a relatively simple rate equation of the form,

$$R_s = A e^{-E/RT} C$$

where C is the mole fraction MTS, R is the gas constant, T is the temperature, E is the activation energy and A is the kinetic rate constant. For R_s in moles/s/cm², A = .0022 and E = 120 kJ/mole. This rate law has given reasonably good fit to experimental densification times using a 1-D CVI model⁸.

A more recent kinetics study shows that the deposition rate also depends on the HCl concentration⁹. This effect becomes more important with increasing reactant depletion. When more is learned about SiC deposition kinetics, a modified reaction expression can be added to the CVI model.

Whatever the deposition rate expression, we still need to know the surface

area function, S_v , in order to calculate the densification rate. For the initial preform the surface area per unit volume depends only on the fiber diameter, D_f , and volume fraction, d_o ,

$$S_v(d_o) = \frac{4d_o}{D_f} \quad (4)$$

and is equal to 1067 cm^{-1} for a preform with 40% v/v of $15 \mu\text{m}$ fiber. At complete densification, $d = 1$, we must have $S_v(1) = 0$. The exact functional form for S_v between these two extremes will depend on the specific fiber architecture. Previous Monte-Carlo simulations of random fiber distributions¹⁰ and geometric analysis for an arrangement of parallel cylinders suggest a function of the form

$$S_v = S^o((1-d)d)^{1/2} \quad (5)$$

where S^o is set using Equation 4 above. This relation likely overestimates the available surface area at high density and does not allow for the formation of closed porosity. A simple linear relationship

$$S_v = S^o(1-d) \quad (6)$$

gives a much lower value of surface area at high density. At this time, little experimental data is available to help choose this relationship. Additional studies of CVI composite microstructures are in progress to better define this parameter.

Heat Flow

In order to calculate the temperature profile, thermal conductivities must be assigned to each of the four types of volume element. For the graphite and porous graphite elements we use 0.15 W/cm/K based on our measurements of "C grade" graphite. This value is also in the range of typical values for the thermal conductivity of stainless steels.

For SiC/Nicalon composites, measured thermal conductivities have been reported over a range of densities both parallel and perpendicular to the cloth layers¹¹. We average these and fit the result to an equation of the form,

$$\frac{1}{k} = \frac{d}{k_1} + \frac{(1-d)}{k_2}$$

where k is the thermal conductivity, and k_1 and k_2 are 1.00 and .032 W/cm/K respectively. This isotropic, density dependent thermal conductivity is used for the preform elements.

For the free space elements, the thermal conductivity is set arbitrarily to a low value of 0.005 W/cm/K.

To complete the thermal model we must also specify the heat capacity of the gas, C_p . We use the temperature dependent heat capacity of hydrogen¹²,

$$C_p = 27.7 + 0.0034 T \text{ (J/mole/K)}$$

as a reasonable approximation.

Gas Flow

In order to calculate the pressure profile and gas flow pattern we must specify gas permeabilities for each type of element. For the two graphite elements and the free space element this is easy; zero for the graphite and "very large" for the free space. We arbitrarily set the "very large" equal to $100 \times 10^{-8} \text{ cm}^2$, an order of magnitude higher than the preform permeability.

For the preform element the gas permeability will depend on density and the specific pore microstructure as densification proceeds. A estimation of this value is given by the Kozeny equation¹³,

$$K = \frac{(1-d)^3}{cS_v^2}$$

which has given reasonable results for many porous materials. The value of S_v is given above and the geometric parameter, c , is taken to be 5.0, within the range of most experimental values. This formula gives a value of $3.8 \times 10^{-8} \text{ cm}^2$ for the initial preform and approaches zero as density approaches 100%.

In addition to the permeability, we must specify the gas viscosity in order to calculate the inlet pressure. We estimate this using the temperature dependent viscosity of hydrogen,

$$\mu = 86 \times 10^{-6} (T/T_0)^{1/2}$$

where μ is the viscosity in poise and $T_0 = 273$ K.

Reactant Transport

The primary mode of reactant transport is by convection in the overall gas flow. Diffusion between volume elements may be significant in regions where the magnitude of the flow is small. For the two graphite elements the effective diffusion coefficient is zero. For the free space element the diffusion coefficient is taken as the binary diffusion coefficient of methane in hydrogen, $0.625 \text{ cm}^2/\text{s}$ at 273 K^{14} . The effective diffusion coefficient for the preform element is calculated from Equation 3 with a tortuosity factor of 2.0.

SIMULATION OF CVI DENSIFICATION

The preform parameters specified above do not correspond to a real preform architecture. In particular the surface area function and the isotropic gas permeability and thermal conductivity functions of the preform element are clearly not applicable to the cloth lay-up preform most often used for CVI-fabricated composites. Even so, these parameters are useful in that they allow us to run the CVI model and to explore the effects of process, transport and kinetic parameters on densification behavior.

Figure 3 shows the fractional density as a function of process time for "baseline" run conditions of 50°C injector temperature, 1200°C furnace temperature, $550 \text{ cm}^3/\text{min}$ of a 9:1 H_2 :MTS gas mixture. Equation 5 is used for S_v . The increase in average density is roughly linear with time, however, the highest density achieved is only 70% of theoretical full density due to the rapid increase in inlet pressure beyond this point. A limit of 200 kPa is used to specify "completion" of the process. The density profile in Figure 4 shows near full density at the hot face of the preform and very little infiltration on the cool side. The densification rate near the hot face is clearly too high to allow uniform densification. Although the densification rate near the cool face increases near the end of the run, it can not "catch up" before the hot face seals off.

The effect of reducing the hot face temperature by 100°C is shown in Figure 5. Although the lower temperature reduces the densification rate near the hot face, the temperature and densification rate on the cool side of the preform also is lower. The overall process time increases somewhat but there is little improvement in density uniformity.

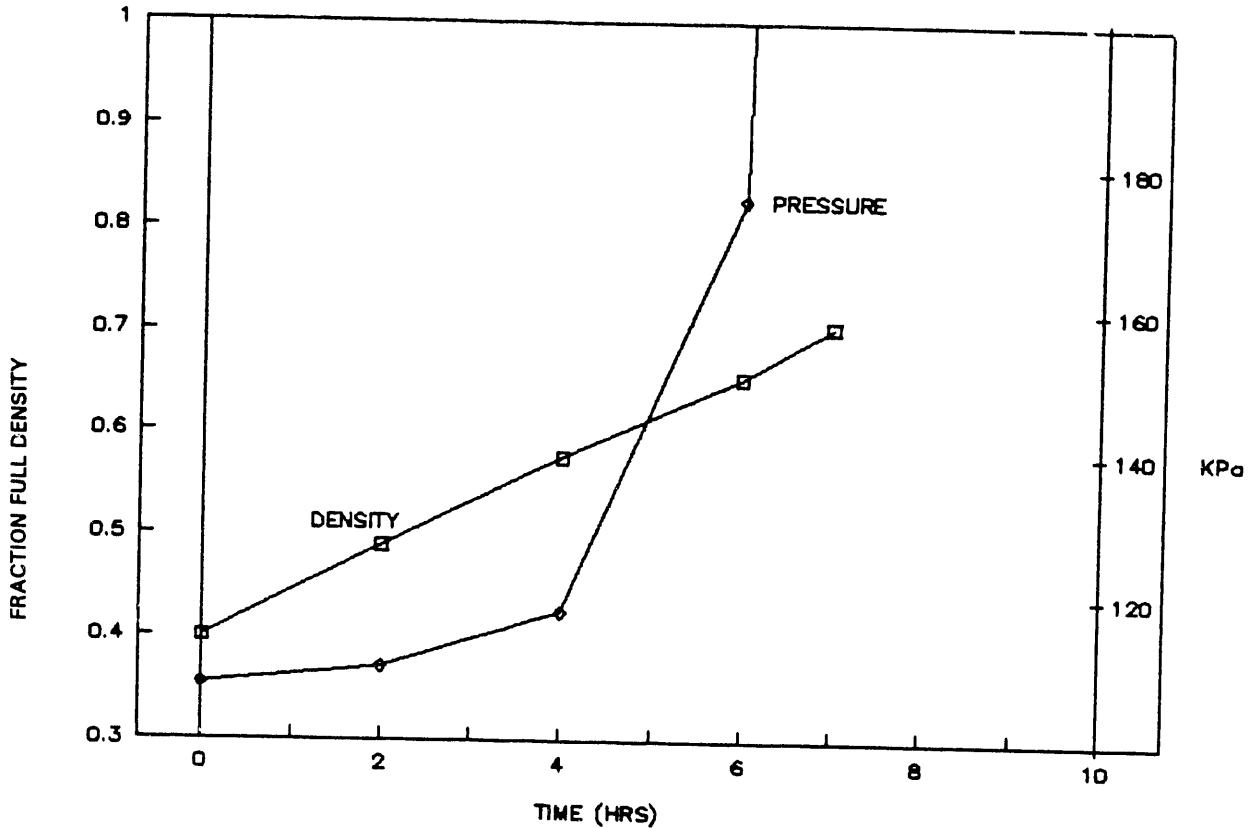


Figure 3. For "baseline" conditions the preform density increases linearly with time and the inlet pressure exceeds 200 kPa after seven hours.

Figure 6 shows the effect of reducing the MTS concentration by 50%. Again, the process time increases by a factor of two but there is no improvement in the average density or its variation through the preform. This result derives directly from the assumption of a simple, first-order rate for the deposition reaction.

Reducing the overall flow rate to 55 cm³/min produces a significant improvement, as shown in Figure 7. The process time is much longer but results in a higher final density and a density profile that is much more uniform. The densification rate near the hot face is reduced due to significant reactant depletion as the gas moves through the preform. Poor densification is still observed near the cool side of the preform at the outer radius.

A different choice for the surface area parameter, S_v , can produce a substantial change in the densification behavior. Using the linear relation (Equation 6) and the "baseline" conditions above, process time increases and the average density and uniformity are greatly improved (Figure 8). The hot face densification rate decreases as density increases, allowing less dense regions to "catch up".

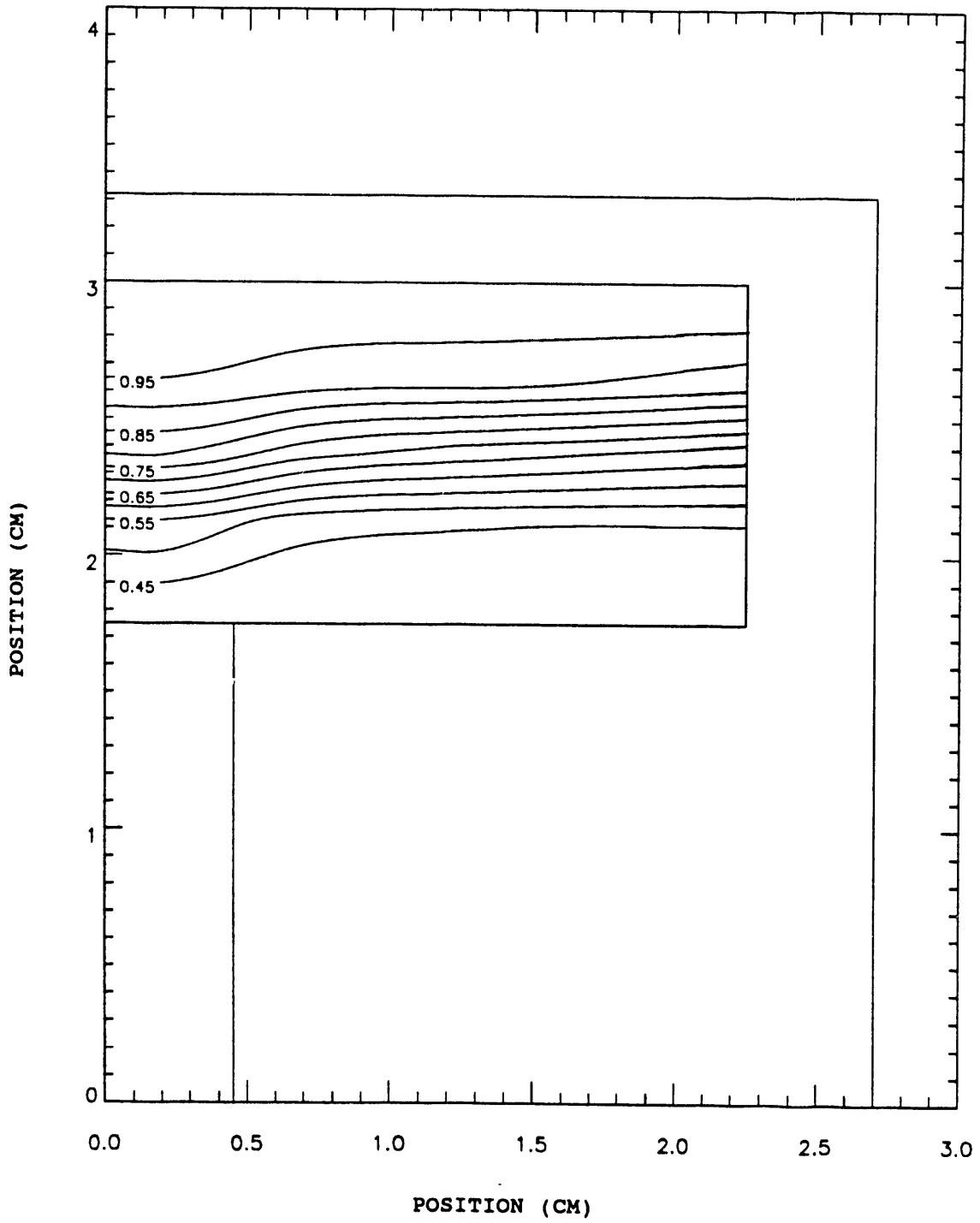


Figure 4. The final density profile for "baseline" conditions shows little densification near the cool face of the preform.

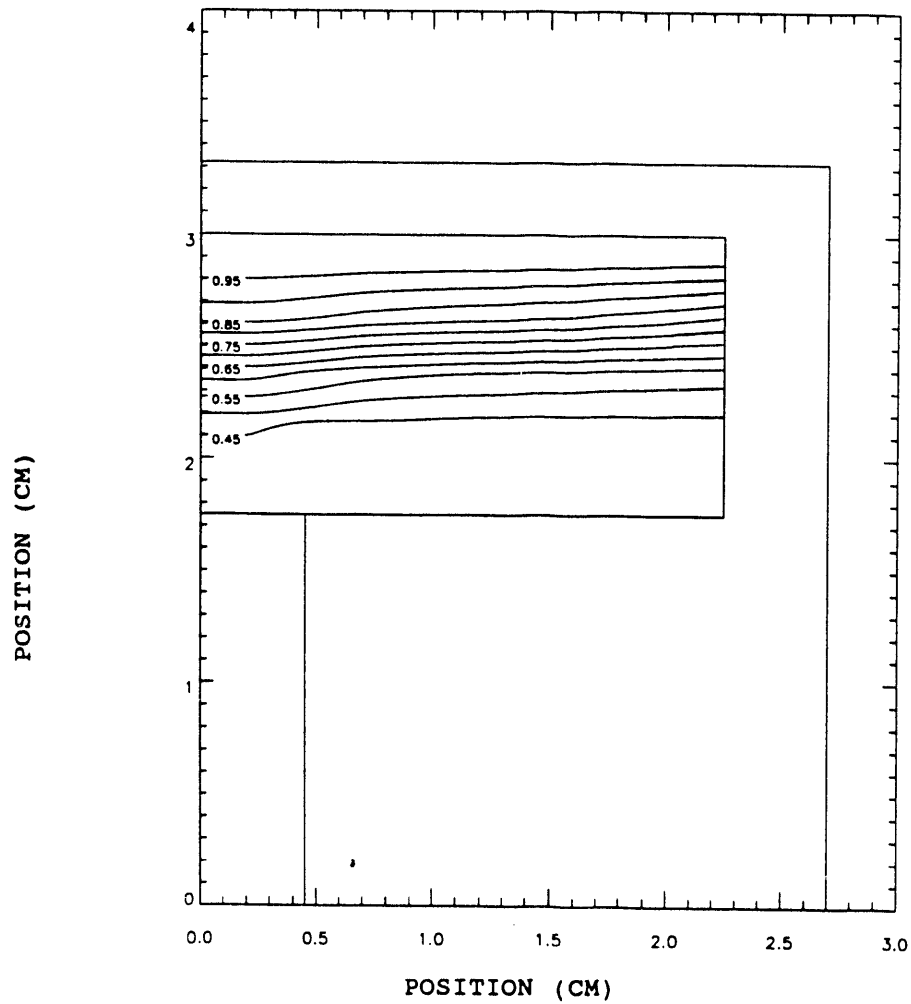
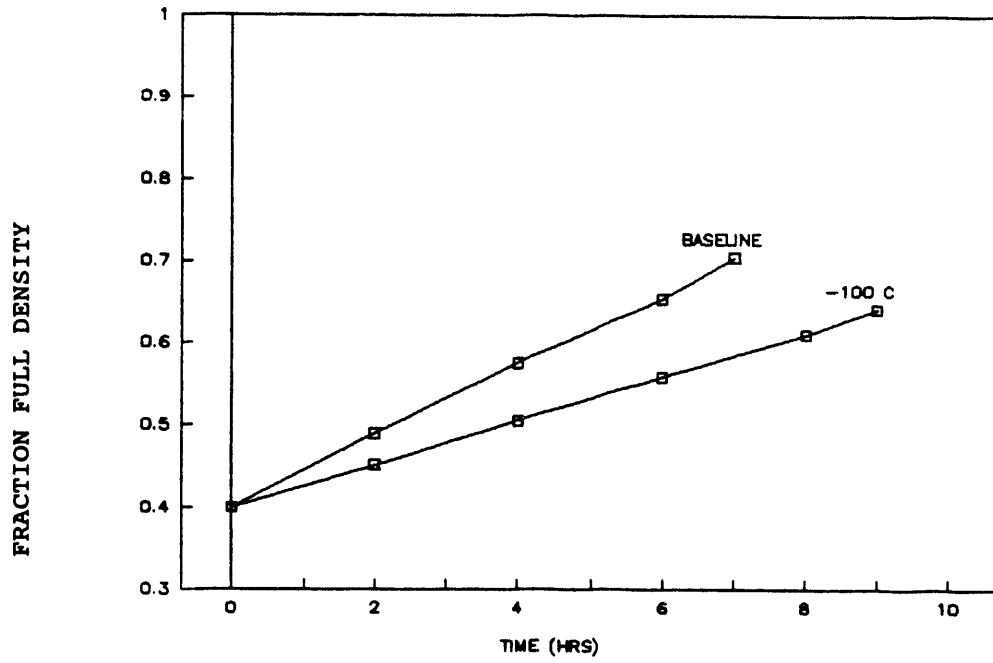


Figure 5. Reducing the hot face temperature increases process time (top) but produces little improvement in density uniformity (bottom).

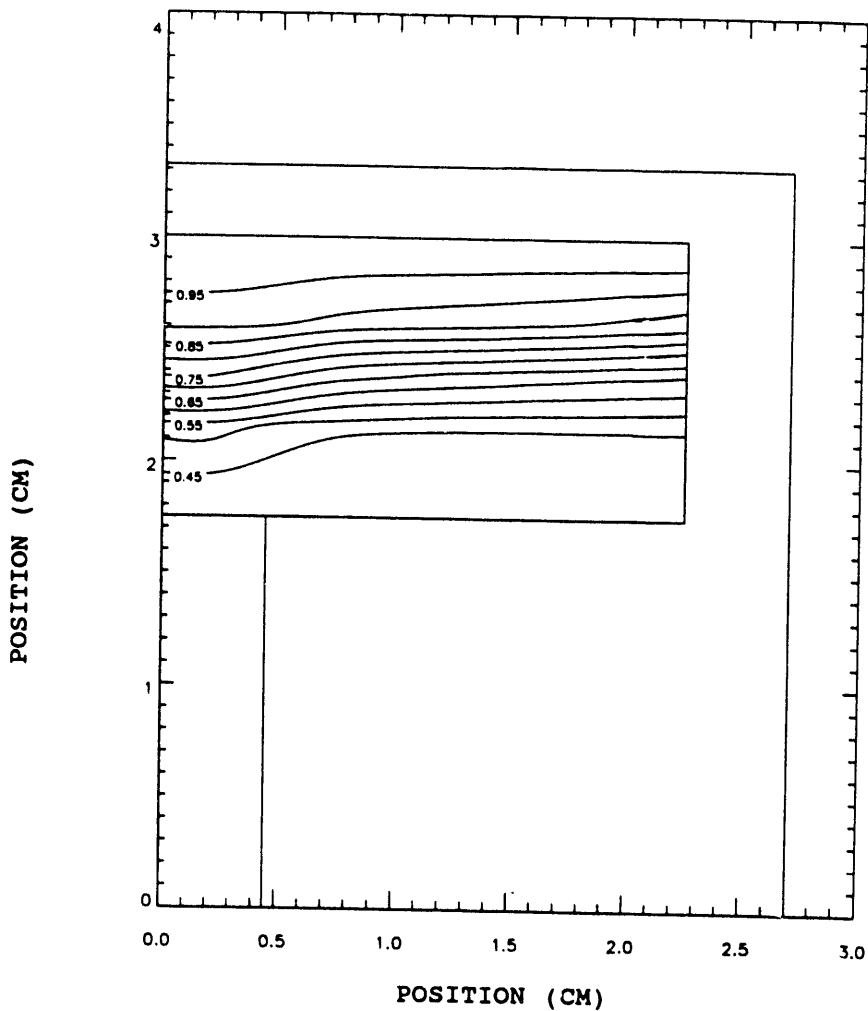
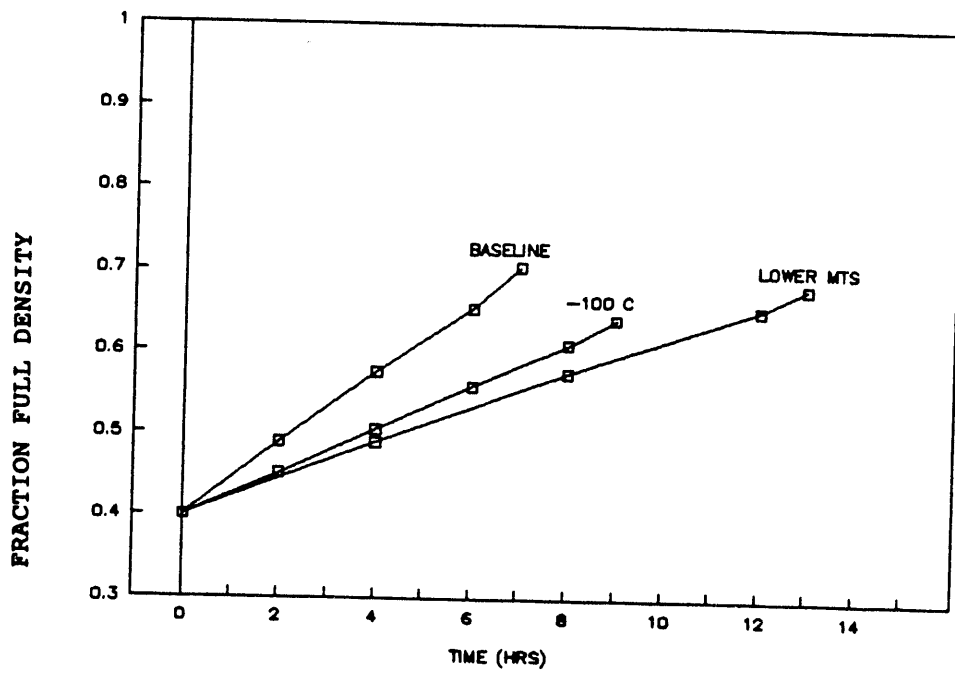


Figure 6. Reducing the MTS concentration increases the process time in inverse proportion (top) but gives no change in the density profile.

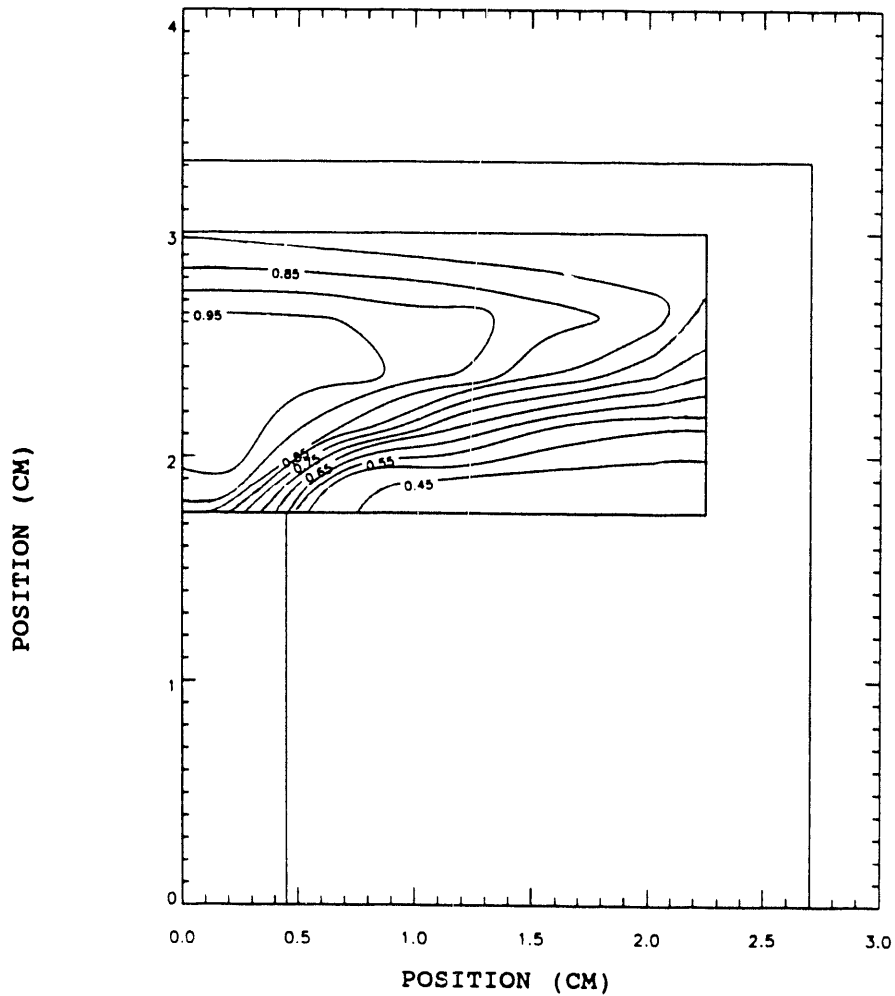
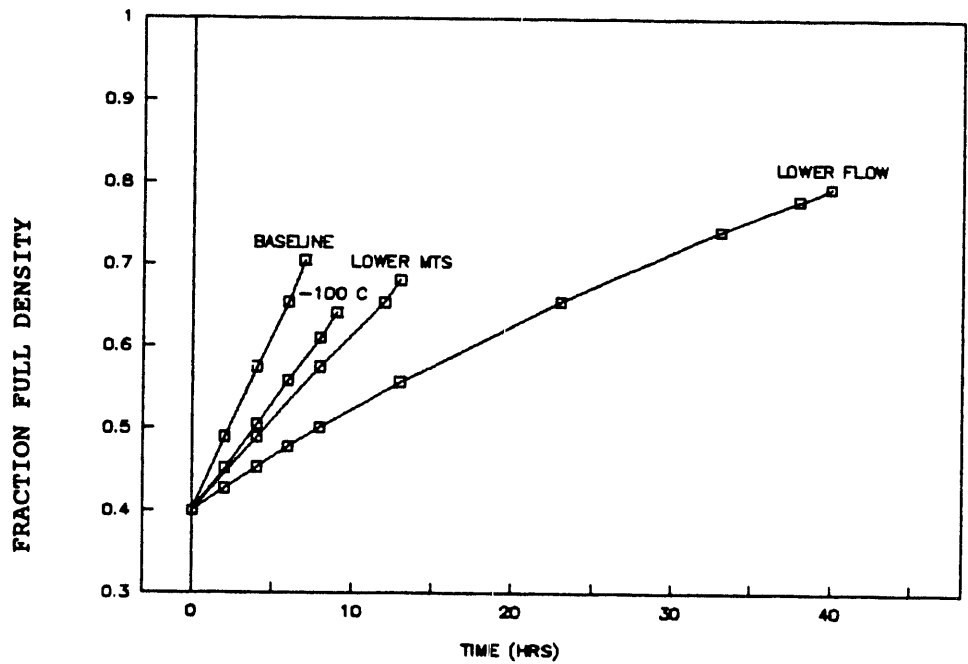


Figure 7. Reducing the overall flow rate give a much longer process time (top) and produces much improved density uniformity (bottom).

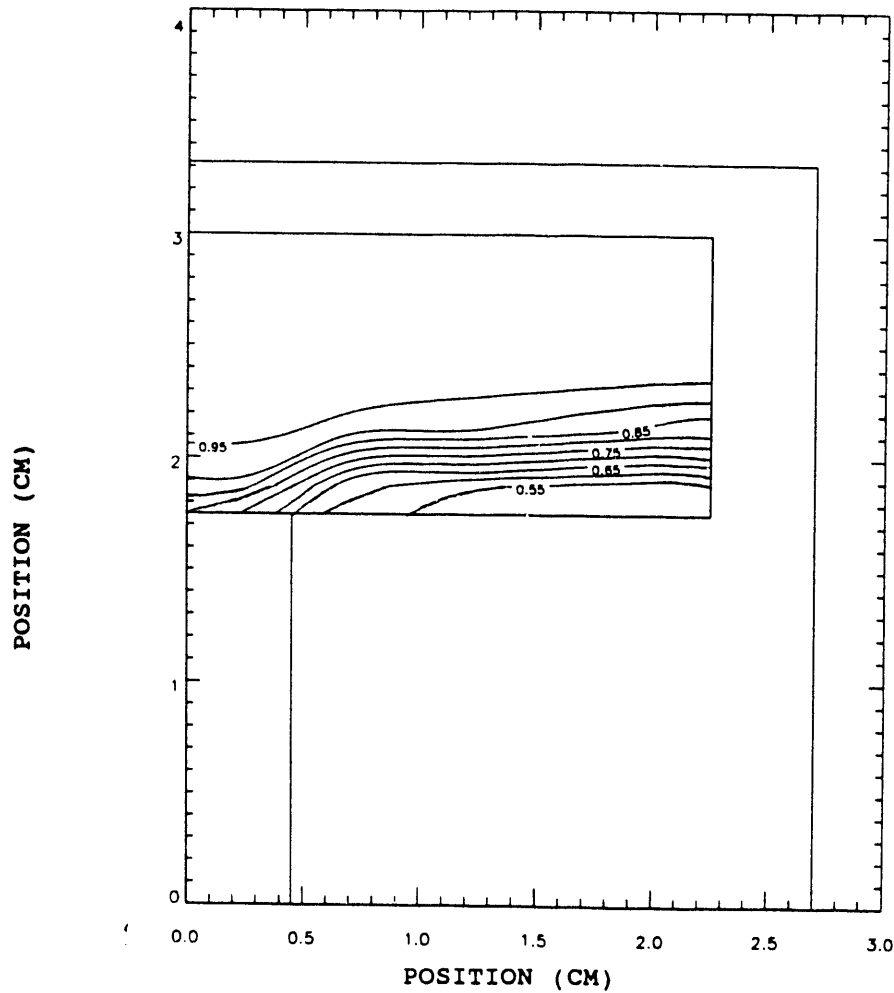
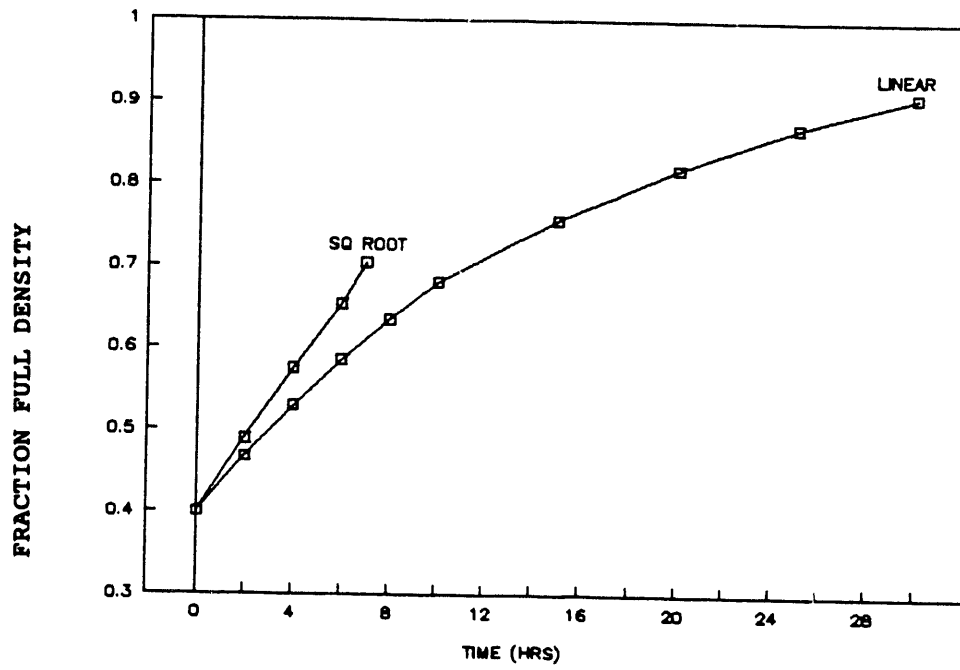


Figure 8. Using the linear surface area relation with "baseline" conditions gives longer process time (top) and more uniform densification (bottom).

SUMMARY AND CONCLUSIONS

A finite volume model for forced flow/thermal gradient CVI has been implemented. The model includes heat transport by conduction and convection, gas flow corresponding to Darcy's Law viscous flow through a permeable body, and transport and reaction of chemical species. Steady-state solutions for temperature, pressure and concentration produce a steady-state densification rate. Time dependent density is produced using an implicit scheme. The densification process is "complete" when the inlet pressure reaches a limiting value.

We believe that this model includes all physical phenomena that are significant to the FCVI process. However, agreement between this simulation and an actual, experimental process will require accurate specification of transport properties and reaction kinetics, and on proper selection of boundary conditions. Significant uncertainty remains with several of these factors. Ongoing measurement efforts at Georgia Tech and at ORNL aim toward better understanding of these for SiC/Nicalon composites and quantitative agreement with experimental processing results.

REFERENCES

1. A. J. Caputo and W. J. Lackey, U.S. Pat. No. 4,580,524 (8 April 1986).
2. A. J. Caputo, W. J. Lackey, and D. P. Stinton, Cer. Eng. Sci. Proc. 6 (7-8), 694-706 (1985).
3. A. J. Caputo, D. P. Stinton, R. A. Lowden, and T. M. Besmann, Am. Ceram. Soc. Bull. 66 (2), 368-72 (1987).
4. T. L. Starr in Proceedings of the Conference on Whisker- and Fiber-Toughened Ceramics, edited by R. A. Bradley, et al. (ASM International, Metals Park, Ohio, 1988) pp. 243-252.
5. S. V. Patankar, Numerical Heat Transfer and Fluid Flow (Hemisphere Publishing Corporation, New York, 1980).
6. D. P. Stinton, private communication, Oak Ridge National Laboratory, Oak Ridge, Tennessee, November 1987.
7. K. Brennfleck, E. Fitzer, B. Schoch, M. Dietrich in Proc. of 9th Int. Conf. on Chemical Vapor Deposition, edited by G.W. Cullen (The Electrochemical Society, Pennington, NJ, 1984) pp. 649-662.
8. T. L. Starr, Modeling of Chemical Vapor Infiltration, Interim Report ORNL/Sub/85-55901/01 prepared for Oak Ridge National Laboratory, U.S. Department of Energy, Contract No. DE-AC05-84OR21400, by the Georgia Tech Research Institute, Georgia Institute of Technology, Atlanta, GA, February, 1989.

9. T. M. Besmann, B. W. Sheldon, and M. D. Kaster, *Surf. Coat. Tech.*, 43/44, 167 (1990).
10. T. L. Starr in Proceedings of the Tenth International Conference on Chemical Vapor Deposition, edited by G.W. Cullen, (The Electrochemical Society, Pennington, NJ, Vol. 87-8, 1988).
11. H. Tawil, L. D. Bentsen, S. Baskaran, D. P. H. Hasselman, *J. Mat. Sci.* 20, 3201-3212 (1985).
12. CRC Handbook of Chemistry and Physics, edited by Robert C. Weast, Melvin J. Astle, and William H. Beyer, 68th Edition, CRC Press, Boca Raton, Florida, 1987-88.
13. J. Kozeny, *Wasserkraft Wasserwirtsch.* 22 67 (1927).
14. Charles N. Satterfield and Thomas K. Sherwood, The Role of Diffusion in Catalysis, Addison-Wesley Publishing Company, Reading, Massachusetts, 1963.

DISTRIBUTION

A.P. GREEN REFRACTORIES COMPANY
Green Blvd.
Mexico, MO 65265
J. L. Hill

AIR PRODUCTS AND CHEMICALS
P.O. Box 538
Allentown, PA 18105
S. W. Dean
S. C. Weiner

ALLISON GAS TURBINE DIVISION
P.O. Box 420
Indianapolis, IN 46206-0420
P. Khandelwal (Speed Code W-5)
R. A. Wenglarz (Speed Code W-16)

AMA RESEARCH & DEVELOPMENT CENTER
5950 McIntyre Street
Golden, CO 80403
T. B. Cox

ARGONNE NATIONAL LABORATORY
9700 S. Cass Avenue
Argonne, IL 60439
W. A. Ellingson
J. P. Singh

ARGONNE NATIONAL LABORATORY-WEST
P.O. Box 2528
Idaho Falls, ID 83403-2528
S. P. Henslee

**ARMY MATERIALS TECHNOLOGY
LABORATORY SLCMT-MCC**
Watertown, MA 02172-0001
D. R. Messier

AVCO RESEARCH LABORATORY
2385 Revere Beach Parkway
Everett, MA 02149
R. J. Pollina

BABCOCK & WILCOX
1562 Beeson St.
Alliance, OH 44601
T. I. Johnson

BABCOCK & WILCOX
Domestic Fossil Operations
20 South Van Buren Avenue
Barberton, OH 44023
M. Gold

BABCOCK & WILCOX
Lynchburg Research Center
P. O. Box 11165
Lynchburg, VA 24506
H. M. Moeller

BATTELLE-COLUMBUS LABORATORIES
505 King Avenue
Columbus, OH 43201
V. K. Sethi

BRITISH COAL CORPORATION
Coal Research Establishment
Stoke Orchard, Cheltenham
Glochester, England GL52 4RZ
M. Arnold
C. Bower
A. Twigg

BRITISH GAS CORPORATION
Westfield Development Center
Cardenden, Fife
Scotland KY50HP
J. E. Scott

BROOKHAVEN NATIONAL LABORATORY
Department of Applied Science
Upton, Long Island, NY 11973
T. E. O'Hare

**CANADA CENTER FOR MINERAL & ENERGY
TECHNOLOGY**
568 Booth Street
Ottawa, Ontario
Canada K1A 0G1
R. Winston Revic
Mahi Sahoo

COLORADO SCHOOL OF MINES
Department of Metallurgical Engineering
Golden, CO 80401
G. R. Edwards

COMBUSTION ENGINEERING
1000 Prospect Hill Road
Windsor, CT 06095
D. A. Canonico

DOW CORNING CORPORATION
3901 S. Saginaw Road
Midland, MI 48686-0995
H. Atwell

EC TECHNOLOGIES
3614 Highpoint Drive
San Antonio, TX 78217
D. J. Kenton

ELECTRIC POWER RESEARCH INSTITUTE
 P.O. Box 10412
 3412 Hillview Avenue
 Palo Alto, CA 94303
 W. T. Bakker
 J. Stringer

EUROPEAN COMMUNITIES JOINT RESEARCH
 CENTRE
 Petten Establishment
 P.O. Box 2
 1755 ZG Petten
 The Netherlands
 M. Van de Voorde

FOSTER WHEELER DEVELOPMENT
 CORPORATION
 Materials Technology Department
 John Blizzard Research Center
 12 Peach Tree Hill Road
 Livingston, NJ 07039
 J. L. Blough

GA TECHNOLOGIES, INC.
 P.O. Box 85608
 San Diego, CA 92138
 T. D. Gulden

IDAHO NATIONAL ENGINEERING
 LABORATORY
 P. O. Box 1625
 Idaho Falls, ID 83415
 D. W. Keefer
 R. B. Loop
 L. A. Lott
 B. H. Rabin

KENNAMETAL, INC.
 Philip McKenna Laboratory
 1011 Old Salem Road
 P. O. Box 639
 Greensburg, PA 15601
 B. North

LANXIDE CORPORATION
 1 Tralee Industrial Park
 Newark, DE 19711
 E. M. Anderson

LAVA CRUCIBLE-REFRACTORIES CO.
 P.O. Box 278
 Zelienople, PA 16063
 T. Mulholland

LAWRENCE LIVERMORE LABORATORY
 P.O. Box 808, L-325
 Livermore, CA 94550
 W. A. Steele

LOS ALAMOS NATIONAL LABORATORY
 P.O. Box 1663
 Los Alamos, NM 87545
 S. R. Skaggs

MASSACHUSETTS INSTITUTE OF
 TECHNOLOGY
 Department of Civil Engineering
 Room I-280, 77 Massachusetts Avenue
 Cambridge, MA 02139
 O. Buyukozturk

NATIONAL INSTITUTE OF STANDARDS AND
 TECHNOLOGY
 Materials Building
 Gaithersburg, MD 20899
 S. J. Dapkunas

NATIONAL MATERIALS ADVISORY BOARD
 National Research Council
 2101 Constitution Avenue
 Washington, DC 20418
 K. M. Zwisky

NEW ENERGY AND INDUSTRIAL
 TECHNOLOGY DEVELOPMENT
 Sunshine 60 Bldg.
 P.O. Box 1151
 1-1 Higashi-Ikebukuro 3-Chrome
 Toshima-Ku, Tokyo, 170
 Japan
 S. Ueda

THE NORTON COMPANY
 High Performance Ceramics Division
 Goddard Road
 Northborough, MA 01532-1545
 N. Corbin

OAK RIDGE NATIONAL LABORATORY
 P.O. Box 2008
 Oak Ridge, TN 37831
 P. T. Carlson
 N. C. Cole
 R. R. Judkins
 J. L. Langford (8 copies)

OFFICE OF NAVAL RESEARCH
 Code 431, 800 N. Quincy Street
 Arlington, VA 22217
 S. G. Fishman

RESEARCH TRIANGLE INSTITUTE
 P. O. Box 12194
 Research Triangle Park, NC 27709
 T. W. Sigmon

SHELL DEVELOPMENT COMPANY
P.O. Box 1380
Houston, TX 77251-1380
L. W. R. Dicks

TENNESSEE VALLEY AUTHORITY
Energy Demonstration & Technology
MR2N58A
Chattanooga, TN 37402-2801
C. M. Huang

3M COMPANY
Ceramic Materials Department
218-3S-04, 3M Center,
St. Paul, MN 55144
L. R. White

THE JOHNS HOPKINS UNIVERSITY
Materials Science & Engineering
Maryland Hall
Baltimore, MD 21218
R. E. Green, Jr.

THE MATERIALS PROPERTIES COUNCIL, INC.
United Engineering Center
345 E. Forty-Seventh Street
New York, NY 10017
M. Prager

THE TORRINGTON COMPANY
Advanced Technology Center
59 Field St.
Torrington, CT 06790
W. J. Chmura

UNION CARBIDE CORPORATION
Linde Division
P.O. Box 44
175 East Park Drive
Tonawanda, NY 14151-0044
Harry Cheung

UNITED TECHNOLOGIES RESEARCH CENTER
MS 24, Silver Lane
East Hartford, CT 06108
K. M. Prewo

UNIVERSITY OF WASHINGTON
Department of Materials Science and
Engineering
101 Wilson, FB-10
Seattle, WA 98195
T. G. Stoebe

VIRGINIA POLYTECHNIC INSTITUTE & STATE
UNIVERSITY
Department of Materials Engineering
Blackburg, VA 24601
J. J. Brown, Jr.
K. L. Reifsnider

WESTINGHOUSE ELECTRIC CORPORATION
Research and Development Center
1310 Beulah Road
Pittsburgh, PA 15235
S. C. Singhal

WESTINGHOUSE HANFORD COMPANY
P.O. Box 1970
W/A-65
Richland, WA 99352
R. N. Johnson

DOE
OAK RIDGE OPERATIONS OFFICE
P.O.Box 2001
Oak Ridge, TN 37831
Assistant Manager for Energy Research and
Development

DOE
OAK RIDGE OPERATIONS OFFICE
Oak Ridge National Laboratory
P. O. Box 2008
Building 4500N, MS 6269
Oak Ridge, TN 37831
E. E. Hoffman

DOE
OFFICE OF BASIC ENERGY SCIENCES
Materials Sciences Division
ER-131 GTN
Washington, DC 20545
J. B. Darby

DOE
OFFICE OF CONSERVATION AND
RENEWABLE ENERGY
CE-12 Forrestal Building
Washington, DC 20545
J. J. Eberhardt

DOE
OFFICE OF FOSSIL ENERGY
Washington, DC 20545
D. J. Beecy (FE-14) GTN
J. P. Carr (FE-14) GTN
F. M. Glaser (FE-14) GTN
T. B. Simpson (FE-25) GTN

DOE
OFFICE OF VEHICLE AND ENERGY R&D
CE-151 Forrestal Building
Washington, DC 20585
R. B. Schulz

DOE
MORGANTOWN ENERGY TECHNOLOGY
CENTER
P.O. Box 880
Morgantown, WV 26505
R. A. Bajura
R. C. Bedick
F. W. Crouse, Jr.
N. T. Holcombe
W. J. Huber
M. J. Mayfield
J. E. Notestein
J. S. Wilson

DOE
PITTSBURGH ENERGY TECHNOLOGY
CENTER
P.O. Box 10940
Pittsburgh, PA 15236
A. H. Baldwin
R. Santore
T. M. Torkos

END

**DATE
FILMED**

01/28/92

